Electronic Research Archive

https://www.aimspress.com/journal/era

ERA, 33(6): 3517–3542.
DOI: 10.3934/era.2025156
Received: 19 March 2025
Revised: 08 May 2025
Accepted: 20 May 2025
Published: 09 June 2025

Research article

Fixed-time synchronization of time-delayed fuzzy memristor-based neural networks: A special exponential function method

Yan Chen[1,2,*], Ravie Chandren Muniyandi[1], Shahnorbanun Sahran[1] and Zuowei Cai[2]

[1] Faculty of Information Science and Technology, Universiti Kebangsaan Malaysia, Bangi 43600, Malaysia
[2] College of Information Science and Technology, Hunan Women's University, Changsha 410002, China

* **Correspondence:** Email: p110494@siswa.ukm.edu.my.

Abstract: This research focuses on controlling fixed-time synchronization (FixTS) in a time-delayed fuzzy memristor-based neural network (TDFMNN). To achieve FixTS and improve convergence speed, a discontinuous state feedback controller (StFC) incorporating a unique exponential function is developed for the memristor-based neural network (MNN) drive-response system (DRS). The FixTS is analyzed using the indefinite derivative Lyapunov function approach. The proposed TDFMNN incorporates multiple factors, such as memristor, time-variation of coefficients, time-delay, and fuzzy elements, making the model more practical compared to existing studies. The StFC is designed using the fixed-time stability (FixS) theory of the exponential function, which requires few parameters, thereby simplifying controller design and implementation. Numerical simulations are conducted to evaluate the performance of the proposed control strategy on two-dimensional and three-dimensional TDMNNs.

Keywords: fixed-time synchronization; fuzzy memristor-based neural network; special exponential function method; state feedback controller; time-delay

1. Introduction

The memristor notion was initially developed by Chua et al. [1] in a study of circuit variables symmetry and logic. However, it became popular in 2008, with the production of the first memristor component in Hewlett-Packard Labs [2]. Memristor circuits demonstrate many important characteristics, such as low power consumption, large memories, nano-scale structure, and non-volatility, making them suitable for numerous applications, including volatile memory, secure communication, analog circuits, image processing, and cryptography. Biological neural network systems inspire artificial neural networks, which are crafted to replicate and simulate the brain's neural structure and learning mechanisms [3]. As the most suitable elements to simulate neuronal synapses [4], using memristors in neural networks not only reduces hardware overhead, system size, and energy consumption, but

also enhances computing speed [4]. This innovation, known as "memristor-based neural networks", outperforms traditional networks in speed, data storage, and performance across various applications [5]. MNNs are considered state-dependent nonlinear switching systems [6]. Investigating their dynamical behavior is crucial for numerous engineering applications. The majority of the current studies focus on stability and synchronization problems to facilitate the application of MNNs [7].

The phenomenon of time delay is unavoidable when studying real network systems [5]. The occurrence of time delays is influenced by both the system's current state and its previous state, which is a more obvious feature in neural networks [8]. There are many reasons for the time delay phenomenon, including the limited signal transmission time between neurons and the insufficient speed of actuators in processing signals [9]. Time delay is one of the most difficult issues to deal with and is widely present in the system, but difficult to eliminate. Therefore, the phenomenon of time delay has attracted significant attention, and extensive research has been undertaken into the delay-dependent stability of delayed systems. [10] proposes a delay-dependent switched system to analyze the stability of delayed systems. The delay in this study [11] addresses the passivity issue in neural networks. This method allows us to incorporate more delay information to construct a novel Lyapunov–Krasovskii functional. Therefore, considering time lags is crucial when examining the dynamics of neural networks. This makes the development of time-delay memristor-based neural network (TMNN) models highly relevant for the dynamic analysis and control of MNNs [12]. The MNN model commonly includes a time-delay term to account for the signal delay due to the effect of switching and the current impedance of the circuit components [13]. The utilization of a TMNN often relies on its synchronization, multi-stability, and other associated dynamic phenomena [14]. As a nonlinear system, the TMNN exhibits complex nonlinear dynamic behaviors. The presence of time lags increases the likelihood of system instability, thereby complicating the implementation of system synchronization and rendering the synchronization process more challenging [15]. The synchronization ensures the interaction between the network nodes and the eventual convergence of their dynamical behaviors to the same state [16].

The synchronization behavior of TMNNs can be classified based on time taken to achieve the synchronization into, infinite-time synchronization (InfTS), finite-time synchronization (FinTS), and FixTS [17]. In the InfTS method, the time required to achieve synchronization cannot be estimated. Notable examples of InfTS synchronization include asymptotic [18] and exponential synchronization [19] of MNNs. However, in many situations, it is important to consider the control cost or time required to achieve system synchronization. FinTS refers to the stability of the error state between the DRS within a finite time. This consideration has led to the introduction of the FinTS method, wherein the duration to reach the synchronization can be estimated [20]. The finite time represents the maximum limit established by the estimated time function, which is determined by the system's initial states (InSts). It corresponds to a synchronization duration achievable within an estimated time range. Nevertheless, the FinTS method is not appropriate for systems whose initial conditions are not readily available [21]. The study by Polyakov [22] introduced a technique to determine if a system can achieve FixS. FixTS, on the other hand, indicates that the system synchronizes within a finite time, with the settling time being bounded concerning the state error, and this upper bound is independent of the InSts of the error system. This technique paved the way for a method of stability analysis that is not reliant on the system's InSts. Therefore, the FixS analysis approach can be applied to FixTS control method. The FixTS analysis method is a special form of FinTS that is not dependent on the InSts of the system and produces a bounded synchronization time (SyTi). FixTS is of great importance

and has numerous practical applications. Due to its strict guarantee on convergence time, FixTS offers significant advantages in safety-critical, dynamically complex, or real-time demanding applications, such as image encryption, aerospace, smart grids, and autonomous driving. However, the issue of FixTS remains relatively immature with many queries requiring further exploration, especially the research on FixTS application in TMNNs.

Recently, many studies considered the characteristics of time delay [23], oscillation [24], and parameter uncertainties [25] to achieve more practical applications with MNNs. However, building an accurate mathematical model representation of an actual engineering application involves a daunting task, due to the fact that ignoring the system's parameter uncertainties can produce adverse effects on the system's dynamics convergence and local stability. Fuzzy logic (FL), proposed by Lotfi Zadeh in 1965, was designed to handle problems involving uncertainty and ambiguity, making it well-suited for nonlinear systems or those that are difficult to model precisely, such as human language or complex control systems. Integrating memristors into FL systems has become a highly prominent research frontier. On one hand, memristors provide compact, energy-efficient, and highly nonlinear components that can physically implement fuzzy operators, store fuzzy rule weights, or emulate synaptic connections in fuzzy neural networks (FNNs). On the other hand, embedding FL into memristive circuits enables the realization of intelligent control strategies capable of addressing system uncertainties, parameter variations, and environmental disturbances. Therefore, this integration opens up new avenues for developing intelligent circuits and systems with enhanced learning, adaptability, and decision-making capabilities, and it is regarded as a promising research direction in the fields of neuromorphic engineering, intelligent control, and hardware-software co-design. The inclusion of fuzzy components enhances the universality and practicality of research on the robust adaptive synchronization of the MNN [26]. This is achieved by addressing the nonlinear properties of the memristor and optimizing the parameter design of the MNN. Therefore, the integration of fuzzy systems holds substantial value in exploring the dynamic analysis of MNNs in the presence of parameter perturbations. Contrary to research on the synchronization of FNNs [27–29] and MNNs, fewer studies have been done on fuzzy MNNs. Given the importance of synchronization behavior, further research on the synchronization of FMNNs is essential [30]. The quality of a control method can be assessed in terms of how quickly it can achieve synchronization. The SyTi of asymptotic synchronization tends to infinity, while the SyTi of FinTS has an upper bound. The FinTS control system may alter control settings in real-time according to the calculated upper limit of the SyTi, enabling the system to quickly achieve synchronization. However, since the upper bound of the SyTi required for FinTS is related to the InSts of the system, it imposes considerable limitations in practical applications.

Compared with the FinTS technique, the convergence time upper limit of the FixTS approach is solely dependent on the control parameters of the system and is independent of InSts. This independence makes it more convenient for practical applications in production and daily life. Therefore, research on the FixTS of TDFMNNs holds more practical significance. However, there is currently limited related research in the literature [31–33], indicating an insufficient resolution to the TDFMNN problem. Most existing FixTS methods involve complex convergence time estimation and extensive computation. This gap motivates us to develop simpler, more effective, and diverse FixTS convergence time estimates. The FixTS control of TDFMNNs remains underexplored, prompting our research.

The innovation of this paper lies in the proposal of TDFMNNs that consider additional objective factors, such as time-delay effects, fuzzy terms, and memristors. The FixS theory based on exponential

functions is applied, involving fewer parameters, which makes the controller easier to design and implement. A special exponential function term is introduced in the modified controller, enabling easier realization of FixTS, with a simpler estimation formula for the convergence time.

This article tries to provide novel FixTS standards for controlling TDFMNNs. The main contributions of this work are summarized as below.

(i) Solved the FixTS problem of TDFMNNs by designing a switching type discontinuous StFC. The inclusion of a special exponential function term in the controller significantly differs from existing power function form controllers, allowing for easier implementation and achieving FixTS more effectively.

(ii) Proposed the TDFMNN model, which integrates multiple factors including nonlinearity, time-variation of coefficients, time-lag, and FL elements, thereby enhancing the model's practicality compared to previous studies [27, 28, 34, 35].

(iii) The StFC controller adopted in this paper utilizes the FixS theory of the exponential function, requiring fewer parameters for controller design and implementation, thus simplifying the process.

(iv) Introduced a novel estimation formula for synchronization convergence time, which is simpler and more practical compared to existing methods, facilitating a more accurate assessment of convergence behaviour.

The structure of the article is as follows: Section 2 delves into the DRS, which are the models under consideration. In addition, the study included the provision of definitions and assumptions, as well as the introduction of valuable lemmas. Section 3 incorporates the FixS theory, and some FixTS criteria and controller designs for TDFMNNs were proposed through rigorous mathematical proof. Section 4 introduces two numerical simulation examples. The fifth section provides a series of findings from this article and proposes some future research work.

Notations: $\mathbb{R}$ represents the real field; $\mathbb{R}^n$ consists of all n-dimensional real vectors; sign$(\cdot)$ is the sign function; $i, j \in N = \{1, 2, ..., n\}$; and $\overline{\text{co}}[E]$ is the convex closure of E. Let $i, j \in \mathbb{R}^n$, (x, y) be the inner product of x and y, and ∂V represent the generalized gradient of V.

2. Model description and preliminaries

Consider the TDFMNNs

$$\begin{aligned}\frac{dx_i(t)}{dt} = &-c_i(t)x_i(t) + \sum_{j=1}^{n} a_{ij}\left(x_i(t)\right)\mathcal{F}_j(x_j(t)) + \sum_{j=1}^{n} b_{ij}\left(x_i(t)\right)\mathcal{G}_j(x_j(t-\sigma)) + \sum_{j=1}^{n} E_{ij}v_j \\ &+ \bigwedge_{j=1}^{n} T_{ij}v_j + \bigwedge_{j=1}^{n} D_{ij}\mathcal{F}_j\left(x_j\left(t-\sigma\right)\right) + \bigvee_{j=1}^{n} H_{ij}\mathcal{F}_j\left(x_j\left(t-\sigma\right)\right) + \bigvee_{j=1}^{n} S_{ij}v_j + I_i,\end{aligned} \tag{1}$$

for $i = 1, 2, ..., n$, where n represents the number of neural network units, $c_i(t) > 0$ reflects the rate by which the potentials will be reset to the equilibrium state in isolation, $x_i(t)$ represents the state variables (StVas) connected to the *ith* neuron, $\mathcal{F}_j(x_j(t)), \mathcal{G}_j(x_j(t-\sigma))$ and $\mathcal{F}_j(x_j(t-\sigma))$ denote the outputs, $\bigwedge$ represent the fuzzy "AND" and $\bigvee$ fuzzy "OR" operations, D_{ij} and H_{ij} represent elements of the fuzzy feedback Min and Max templates, respectively, T_{ij} and S_{ij} denote the fuzzy feed-forward Min template and Max template, respectively, the fuzzy feed-forward template is E_{ij}, v_i and I_i are the input and bias, respectively and the memristor-based weights $a_{ij}(x_i(t))$ and $b_{ij}(x_i(t))$ can be defined as follows:

$$a_{ij}(x_i(t)) = \begin{cases} \hat{a}_{ij}, & |x_i(t)| \le r_i, \\ \check{a}_{ij}, & |x_i(t)| > r_i, \end{cases} \tag{2}$$

$$b_{ij}(x_i(t)) = \begin{cases} \hat{b}_{ij}, & |x_i(t)| \le r_i, \\ \check{b}_{ij}, & |x_i(t)| > r_i, \end{cases} \tag{3}$$

where $r_i > 0$ is a switching jump, and $\hat{a}_{ij}, \check{a}_{ij}, \hat{b}_{ij}, \check{b}_{ij}$ are constants associated with memristors.

Lemma 2.1. *(Refer to Corollary 1 of [36]). Assume that $\varnothing \in k_\infty$, and let $l > 0$, $0 < q < 1$ be given constants. Suppose there exists a locally Lipschitz continuous and C-regular function $V : \mathbb{R}^n \to \mathbb{R}_+$ such that $V(0) = 0$, and the following conditions are satisfied:*

$$\frac{dV}{dt} \le -l \exp\left(V^q\right) V^{1-q}.$$

The zero point of the equation remains stable at a constant time, and the convergence time is estimated as $\Gamma(t_0, x_0) \le t_0 + \Gamma^{\max}, \Gamma^{\max} = \frac{1}{ql}$.

Lemma 2.2. *(Chain Rule [37, 38]). If $V : \mathbb{R}^n \to \mathbb{R}$ is C- regular and $x(t) : [t_0, +\infty) \to \mathbb{R}^n$ has absolute continuity, then*

$$\frac{dV(x(t))}{dt} =< \ell(t), \frac{dx(t)}{dt} >, \forall \ell(t) \in \partial V(x(t)).$$

Lemma 2.3. *(Refer to [39]). Let x and $\tilde{x}$ denote the states of system (1). Then, we can conclude that:*

$$\left| \bigwedge_{j=1}^{n} D_{ij}\mathcal{F}_j(x_j) - \bigwedge_{j=1}^{n} D_{ij}\mathcal{F}_j(\tilde{x}_j) \right| \le \sum_{j=1}^{n} |D_{ij}||\mathcal{F}_j(x_j) - \mathcal{F}_j(\tilde{x}_j)|,$$

$$\left| \bigvee_{j=1}^{n} H_{ij}\mathcal{F}_j(x_j) - \bigvee_{j=1}^{n} H_{ij}\mathcal{F}_j(\tilde{x}_j) \right| \le \sum_{j=1}^{n} |H_{ij}||\mathcal{F}_j(x_j) - \mathcal{F}_j(\tilde{x}_j)|.$$

To reach the conclusion of this article, the following conditions are considered.

(A1) The functions $\mathcal{F}_j$ and $\mathcal{G}_j$ satisfy $\mathcal{F}_j(0) = \mathcal{G}_j(0) = 0, \forall x, y \in \mathbb{R}$, and we can find $P_j > 0, Q_j > 0, j = 1, 2, \ldots, n$ satisfying

$$\begin{aligned} P_j|x - y| &\ge |\mathcal{F}_j(x) - \mathcal{F}_j(y)|, \\ Q_j|x - y| &\ge |\mathcal{G}_j(x) - \mathcal{G}_j(y)|. \end{aligned} \tag{4}$$

(A2) For any pair of distinct real numbers x and y, we can find $L_j > 0$ and $M_j > 0$ that satisfy the following inequality:

$$\begin{aligned} |\mathcal{F}_j(x)| &\le L_j, \\ |\mathcal{G}_j(x)| &\le M_j. \end{aligned} \tag{5}$$

Utilizing the Filippov-framework theorem, it is deduced from (1) that

$$\begin{aligned}\frac{dx_i(t)}{dt} \in & -c_i(t)x_i(t) + \sum_{j=1}^{n} \overline{\text{co}}\left[a_{ij}\left(x_i(t)\right)\right]\mathcal{F}_j(x_j(t)) + \sum_{j=1}^{n} \overline{\text{co}}\left[b_{ij}\left(x_i(t)\right)\right]\mathcal{G}_j(x_j(t-\sigma)) + \sum_{j=1}^{n} E_{ij}v_j \\ & + \bigwedge_{j=1}^{n} T_{ij}v_j + \bigwedge_{j=1}^{n} D_{ij}\mathcal{F}_j(x_j(t-\sigma)) + \bigvee_{j=1}^{n} H_{ij}\mathcal{F}_j(x_j(t-\sigma)) + \bigvee_{j=1}^{n} S_{ij}v_j + I_i,\end{aligned} \tag{6}$$

where

$$\overline{\text{co}}[a_{ij}(x_i(t))] = \begin{cases} \hat{a}_{ij}, & r_i > |x_i(t)|, \\ \left[\underline{a}_{ij}, \bar{a}_{ij}\right], & r_i = |x_i(t)|, \\ \check{a}_{ij}, & r_i < |x_i(t)|, \end{cases} \tag{7}$$

$$\underline{a}_{ij} = \min\{\hat{a}_{ij}, \check{a}_{ij}\}, \quad \overline{a}_{ij} = \max\{\hat{a}_{ij}, \check{a}_{ij}\},$$

and

$$\overline{\text{co}}[b_{ij}(x_i(t))] = \begin{cases} \hat{b}_{ij}, & r_i > |x_i(t)|, \\ \left[\underline{b}_{ij}, \bar{b}_{ij}\right], & r_i = |x_i(t)|, \\ \check{b}_{ij}, & r_i < |x_i(t)|, \end{cases} \tag{8}$$

$$\underline{b}_{ij} = \min\{\hat{b}_{ij}, \check{b}_{ij}\}, \quad \overline{b}_{ij} = \max\{\hat{b}_{ij}, \check{b}_{ij}\}.$$

For $i, j \in \mathbb{N}$, we can find $\alpha_{ij}(t) \in \overline{\text{co}}[a_{ij}(x_i(t))]$ and $\beta_{ij}(t) \in \overline{\text{co}}[b_{ij}(x_i(t))]$ for a.e. $t \geq 0$ to make

$$\begin{aligned}\frac{dx_i(t)}{dt} = & -c_i(t)x_i(t) + \sum_{j=1}^{n} \alpha_{ij}(t)\mathcal{F}_j(x_j(t)) + \sum_{j=1}^{n} \beta_{ij}(t)\mathcal{G}_j(x_j(t-\sigma)) + \sum_{j=1}^{n} E_{ij}v_j \\ & + \bigwedge_{j=1}^{n} T_{ij}v_j + \bigwedge_{j=1}^{n} D_{ij}\mathcal{F}_j(x_j(t-\sigma)) + \bigvee_{j=1}^{n} H_{ij}\mathcal{F}_j(x_j(t-\sigma)) + \bigvee_{j=1}^{n} S_{ij}v_j + I_i.\end{aligned} \tag{9}$$

Applying the drive-response synchronization principle and employing (1) as the drive system (DrSy), the response system (ReSy) is constructed as

$$\begin{aligned}\frac{dy_i(t)}{dt} = & -c_i(t)y_i(t) + \sum_{j=1}^{n} a_{ij}\left(y_i(t)\right)\mathcal{F}_j(y_j(t)) + \sum_{j=1}^{n} b_{ij}\left(y_i(t)\right)\mathcal{G}_j(y_j(t-\sigma)) + \sum_{j=1}^{n} E_{ij}v_j \\ & + \bigwedge_{j=1}^{n} T_{ij}v_j + \bigwedge_{j=1}^{n} D_{ij}\mathcal{F}_j(y_j(t-\sigma)) + \bigvee_{j=1}^{n} H_{ij}\mathcal{F}_j(y_j(t-\sigma)) + \bigvee_{j=1}^{n} S_{ij}v_j + I_i + u_i(t),\end{aligned} \tag{10}$$

where $u_i(t)$ is the proposed controller under development, while the rest of the parameters retain their dynamic interpretations as in (1), and

$$a_{ij}(y_i(t)) = \begin{cases} \hat{a}_{ij}, & |y_i(t)| \leq r_i, \\ \check{a}_{ij}, & |y_i(t)| > r_i, \end{cases} \tag{11}$$

$$b_{ij}(y_i(t)) = \begin{cases} \hat{b}_{ij}, & |y_i(t)| \le r_i, \\ \check{b}_{ij}, & |y_i(t)| > r_i. \end{cases} \tag{12}$$

From Eq (10), it can be deduced that with the implementation of the aforementioned principles:

$$\begin{aligned} \frac{dy_i(t)}{dt} \in & -c_i(t)y_i(t) + \sum_{j=1}^{n} \overline{\text{co}}\left[a_{ij}\left(y_i(t)\right)\right]\mathcal{F}_j(y_j(t)) + \sum_{j=1}^{n} \overline{\text{co}}\left[b_{ij}\left(y_i(t)\right)\right]\mathcal{G}_j(y_j(t-\sigma)) + \sum_{j=1}^{n} E_{ij}v_j \\ & + \bigwedge_{j=1}^{n} T_{ij}v_j + \bigwedge_{j=1}^{n} D_{ij}\mathcal{F}_j(y_j(t-\sigma)) + \bigvee_{j=1}^{n} H_{ij}\mathcal{F}_j(y_j(t-\sigma)) + \bigvee_{j=1}^{n} S_{ij}v_j + I_i + u_i(t), \end{aligned} \tag{13}$$

where

$$\overline{\text{co}}[a_{ij}(y_i(t))] = \begin{cases} \hat{a}_{ij}, & r_i > |y_i(t)|, \\ \left[\underline{a}_{ij}, \bar{a}_{ij}\right], & r_i = |y_i(t)|, \\ \check{a}_{ij}, & r_i < |y_i(t)|, \end{cases} \tag{14}$$

$$\underline{a}_{ij} = \min\{\hat{a}_{ij}, \check{a}_{ij}\}, \quad \overline{a}_{ij} = \max\{\hat{a}_{ij}, \check{a}_{ij}\},$$

and

$$\overline{\text{co}}[b_{ij}(y_i(t))] = \begin{cases} \hat{b}_{ij}, & r_i > |y_i(t)|, \\ \left[\underline{b}_{ij}, \bar{b}_{ij}\right], & r_i = |y_i(t)|, \\ \check{b}_{ij}, & r_i < |y_i(t)|, \end{cases} \tag{15}$$

$$\underline{b}_{ij} = \min\{\hat{b}_{ij}, \check{b}_{ij}\}, \quad \overline{b}_{ij} = \max\{\hat{b}_{ij}, \check{b}_{ij}\}.$$

For $i, j \in \mathbb{N}$, we can find $\tilde{\alpha}_{ij}(t) \in \overline{\text{co}}[a_{ij}(y_i(t))]$ and $\tilde{\beta}_{ij}(t) \in \overline{\text{co}}[b_{ij}(y_i(t))]$ for a.e. $t \ge 0$ satisfying

$$\begin{aligned} \frac{dy_i(t)}{dt} = & -c_i(t)y_i(t) + \sum_{j=1}^{n} \tilde{\alpha}_{ij}(t)\mathcal{F}_j(y_j(t)) + \sum_{j=1}^{n} \tilde{\beta}_{ij}(t)\mathcal{G}_j(y_j(t-\sigma)) + \sum_{j=1}^{n} E_{ij}v_j \\ & + \bigwedge_{j=1}^{n} T_{ij}v_j + \bigwedge_{j=1}^{n} D_{ij}\mathcal{F}_j\left(y_j(t-\sigma)\right) + \bigvee_{j=1}^{n} H_{ij}\mathcal{F}_j\left(y_j(t-\sigma)\right) + \bigvee_{j=1}^{n} S_{ij}v_j + I_i + u_i(t). \end{aligned} \tag{16}$$

The initial values of the Eqs (1) and (6) are $\phi(s) \in C([-\sigma, 0], \mathbb{R}^n)$ and $\Psi(s) \in C([-\sigma, 0], \mathbb{R}^n)$, respectively.

3. Synchronization analysis

Here, a criterion is constructed to ensure the FixTS of the discontinuous DrSy (1) and the discontinuous ReSy (10).

Let $e_i(t) = y_i(t) - x_i(t)$. If $x(t)$ and $y(t)$ are two arbitrary solutions to (1) and (10), respectively, the error dynamic can be obtained as follows:

$$\begin{aligned}\frac{de_i(t)}{dt} &= -c_i(t)e_i(t) + \sum_{j=1}^{n}\alpha_{ij}(t)\tilde{\mathcal{F}}_j(e_j(t)) + \sum_{j=1}^{n}\beta_{ij}(t)\tilde{\mathcal{G}}_j(e_j(t-\sigma)) + \sum_{j=1}^{n}(\tilde{\alpha}_{ij}(t)-\alpha_{ij}(t))\mathcal{F}_j(y_j(t)) \\ &+ \sum_{j=1}^{n}(\tilde{\beta}_{ij}(t)-\beta_{ij}(t))\mathcal{G}_j(y_j(t-\sigma)) + \bigwedge_{j=1}^{n} D_{ij}\mathcal{F}_j(y_j(t-\sigma)) - \bigwedge_{j=1}^{n} D_{ij}\mathcal{F}_j(x_j(t-\sigma)) \\ &+ \bigvee_{j=1}^{n} H_{ij}\mathcal{F}_j(y_j(t-\sigma)) - \bigvee_{j=1}^{n} H_{ij}\mathcal{F}_j(x_j(t-\sigma)) + u_i(t),\end{aligned} \tag{17}$$

where

$$\tilde{\mathcal{F}}_j(e_j(t)) = \mathcal{F}_j(y_j(t)) - \mathcal{F}_j(x_j(t)),$$

$$\tilde{\mathcal{G}}_j(e_j(t-\sigma)) = \mathcal{G}_j(y_j(t-\sigma)) - \mathcal{G}_j(x_j(t-\sigma)).$$

Design a control strategy

$$u_i(t) = -\delta_i e_i(t) - \omega_i \cdot \operatorname{sign}(e_i(t)) - \sum_{j=1}^{n} k_{ij}\left|e_j(t-\sigma)\right| \cdot \operatorname{sign}(e_i(t)) - \Gamma(t,e)\left|e_i(t)\right|^{1-q} \cdot \operatorname{sign}(e_i(t)), \tag{18}$$

where

$$\Gamma(t,e) = l\exp\left(\left(\sum_{i=1}^{n} e_i(t)\right)^q\right),$$

δ_i, ω_i, and k_{ij} are the control parameters, and $0 < q < 1, l > 1$ are positive constants.

Remark 3.1. *In the modified controller, a specially designed exponential function term is introduced, which is noticeably different from the conventional power-function-based controllers. This optimized controller enables FixTS more readily, and the estimation of the convergence time becomes simpler. From the perspective of neural network circuit implementation, such an optimized controller is also easier to realize and entails lower economic costs.*

The key findings of this research can be demonstrated as follows:

Theorem 3.1. *Given that (A1) and (A2) hold, if the conditions*
(i) $\delta_i + c_i(t) - \sum_{j=1}^{n} a_{ji}^D P_j \geq 0$,
(ii) $\omega_i - \sum_{j=1}^{n}\left|\hat{a}_{ij} - \check{a}_{ij}\right| L_j - \sum_{j=1}^{n}\left|\hat{b}_{ij} - \check{b}_{ij}\right| M_j \geq 0$,
(iii) $k_{ij} - b_{ij}^D Q_j - \left|D_{ij}\right| P_j - \left|H_{ij}\right| P_j \geq 0$,
are satisfied, then the ReSy (10) is synchronized with the DrSy (1) in a fixed time under control strategy (18).

Proof. Consider the Lyapunov function

$$V(t) = \sum_{i=1}^{n}\left|e_i(t)\right|. \tag{19}$$

The derivative of $V(t)$ can be defined as

$$\begin{aligned}
\frac{dV(t)}{dt} &= \sum_{i=1}^{n} \frac{de_i(t)}{dt} \cdot \text{sign}(e_i(t)) \\
&= \sum_{i=1}^{n} \Big[- c_i(t)e_i(t) + \sum_{j=1}^{n} \alpha_{ij}(t)\tilde{\mathcal{F}}_j(e_j(t)) + \sum_{j=1}^{n} \beta_{ij}(t)\tilde{\mathcal{G}}_j(e_j(t-\sigma)) + \sum_{j=1}^{n} (\tilde{\alpha}_{ij}(t) - \alpha_{ij}(t))\mathcal{F}_j(y_j(t)) \\
&\quad + \sum_{j=1}^{n} (\tilde{\beta}_{ij}(t) - \beta_{ij}(t))\mathcal{G}_j(y_j(t-\sigma)) + \bigwedge_{j=1}^{n} D_{ij}\mathcal{F}_j(y_j(t-\sigma)) - \bigwedge_{j=1}^{n} D_{ij}\mathcal{F}_j(x_j(t-\sigma)) \\
&\quad + \bigvee_{j=1}^{n} H_{ij}\mathcal{F}_j(y_j(t-\sigma)) - \bigvee_{j=1}^{n} H_{ij}\mathcal{F}_j(x_j(t-\sigma)) + u_i(t) \Big] \cdot \text{sign}(e_i(t)) \\
&\leq - \sum_{i=1}^{n} c_i(t)|e_i(t)| + \sum_{i=1}^{n}\sum_{j=1}^{n} |\alpha_{ij}(t)||\tilde{\mathcal{F}}_j(e_j(t))| + \sum_{i=1}^{n}\sum_{j=1}^{n} |\beta_{ij}(t)||\tilde{\mathcal{G}}_j(e_j(t-\sigma))| \cdot |\text{sign}(e_i(t))| \\
&\quad + \sum_{i=1}^{n}\sum_{j=1}^{n} |\tilde{\alpha}_{ij}(t) - \alpha_{ij}(t)||\mathcal{F}_j(y_j(t))| \cdot |\text{sign}(e_i(t))| \\
&\quad + \sum_{i=1}^{n}\sum_{j=1}^{n} |\tilde{\beta}_{ij}(t) - \beta_{ij}(t)|\mathcal{G}_j(y_j(t-\sigma))| \cdot |\text{sign}(e_i(t))| \\
&\quad + \sum_{i=1}^{n} |\bigwedge_{j=1}^{n} D_{ij}\mathcal{F}_j(y_j(t-\sigma)) - \bigwedge_{j=1}^{n} D_{ij}\mathcal{F}_j(x_j(t-\sigma))| \cdot |\text{sign}(e_i(t))| \\
&\quad + \sum_{i=1}^{n} |\bigvee_{j=1}^{n} H_{ij}\mathcal{F}_j(y_j(t-\sigma)) - \bigvee_{j=1}^{n} H_{ij}\mathcal{F}_j(x_j(t-\sigma))| \cdot |\text{sign}(e_i(t))| \\
&\quad + \sum_{j=1}^{n} u_i(t) \cdot |\text{sign}(e_i(t))|.
\end{aligned} \tag{20}$$

It is shown from (A1, A2) that

$$\sum_{i=1}^{n}\sum_{j=1}^{n} |\alpha_{ij}(t)||\tilde{\mathcal{F}}_j(e_j(t))| \leq \sum_{i=1}^{n}\sum_{j=1}^{n} a_{ji}^{D} P_j |e_i(t)|, \tag{21}$$

where

$$a_{ji}^{D} = \max\{|\underline{a}_{ji}|, |\overline{a}_{ji}|\}.$$

$$\begin{aligned}
&\sum_{i=1}^{n}\sum_{j=1}^{n} |\beta_{ij}(t)||\tilde{\mathcal{G}}_j(e_j(t-\sigma))| \cdot |\text{sign}(e_i(t))| \\
&\leq \sum_{i=1}^{n}\sum_{j=1}^{n} b_{ij}^{D} Q_j |e_j(t-\sigma)| \cdot |\text{sign}(e_i(t))|,
\end{aligned} \tag{22}$$

where

$$b_{ij}^{D} = \max\{|\underline{b}_{ij}|, |\overline{b}_{ij}|\}.$$

$$\begin{aligned}&\sum_{i=1}^{n}\sum_{j=1}^{n}|\tilde{\alpha}_{ij}(t)-\alpha_{ij}(t)||\mathcal{F}_j(y_j(t))|\cdot|\text{sign}(e_i(t))|\\&\leq\sum_{i=1}^{n}\sum_{j=1}^{n}\left|\hat{a}_{ij}-\check{a}_{ij}\right|L_j\cdot|\text{sign}(e_i(t))|.\end{aligned}\tag{23}$$

$$\begin{aligned}&\sum_{i=1}^{n}\sum_{j=1}^{n}|\tilde{\beta}_{ij}(t)-\beta_{ij}(t)||\mathcal{G}_j(y_j(t-\sigma))|\cdot|\text{sign}(e_i(t))|\\&\leq\sum_{i=1}^{n}\sum_{j=1}^{n}\left|\hat{b}_{ij}-\check{b}_{ij}\right|M_j\cdot|\text{sign}(e_i(t))|.\end{aligned}\tag{24}$$

$$\begin{aligned}&\sum_{i=1}^{n}\left|\bigwedge_{j=1}^{n}D_{ij}\mathcal{F}_j(y_j(t-\sigma))-\bigwedge_{j=1}^{n}D_{ij}\mathcal{F}_j(x_j(t-\sigma))\right|\cdot|\text{sign}(e_i(t))|\\&\leq\sum_{i=1}^{n}\sum_{j=1}^{n}|D_{ij}||\mathcal{F}_j(y_j(t-\sigma))-\mathcal{F}_j(x_j(t-\sigma))|\cdot|\text{sign}(e_i(t))|\\&\leq\sum_{i=1}^{n}\sum_{j=1}^{n}|D_{ij}|P_j|(e_j(t-\sigma))|\cdot|\text{sign}(e_i(t))|.\end{aligned}\tag{25}$$

$$\begin{aligned}&\sum_{i=1}^{n}\left|\bigvee_{j=1}^{n}H_{ij}\mathcal{F}_j(y_j(t-\sigma))-\bigvee_{j=1}^{n}H_{ij}\mathcal{F}_j(x_j(t-\sigma))\right|\cdot|\text{sign}(e_i(t))|\\&\leq\sum_{i=1}^{n}\sum_{j=1}^{n}|H_{ij}||\mathcal{F}_j(y_j(t-\sigma))-\mathcal{F}_j(x_j(t-\sigma))|\cdot|\text{sign}(e_i(t))|\\&\leq\sum_{i=1}^{n}\sum_{j=1}^{n}|H_{ij}|P_j|(e_j(t-\sigma))|\cdot|\text{sign}(e_i(t))|.\end{aligned}\tag{26}$$

Substituting (21)–(26) into (20), we obtain

$$\begin{aligned}\frac{dV(t)}{dt}\leq&-\sum_{i=1}^{n}[c_i(t)-\sum_{j=1}^{n}a_{ji}^{D}P_j]|e_i(t)|\\&+\sum_{i=1}^{n}\sum_{j=1}^{n}b_{ij}^{D}Q_j|e_j(t-\sigma)|\cdot|\text{sign}(e_i(t))|\end{aligned}$$

$$
\begin{aligned}
&+\sum_{i=1}^{n}\sum_{j=1}^{n}(\left|\hat{a}_{ij}-\check{a}_{ij}\right|L_j+\left|\hat{b}_{ij}-\check{b}_{ij}\right|M_j)\cdot|\mathrm{sign}(e_i(t))|\\
&+\sum_{i=1}^{n}\sum_{j=1}^{n}|D_{ij}|P_j|(e_j(t-\sigma))|\cdot|\mathrm{sign}(e_i(t))|\\
&+\sum_{i=1}^{n}\sum_{j=1}^{n}|H_{ij}|P_j|(e_j(t-\sigma))|\cdot|\mathrm{sign}(e_i(t))|\\
&+\sum_{i=1}^{n}u_i(t)\cdot|\mathrm{sign}(e_i(t))|. \qquad (27)
\end{aligned}
$$

Substituting (18) into (27), we obtain

$$
\begin{aligned}
\frac{dV(t)}{dt}\le&-\sum_{i=1}^{n}[c_i(t)-\sum_{j=1}^{n}a_{ji}^{D}P_j]|e_i(t)|\\
&+\sum_{i=1}^{n}\sum_{j=1}^{n}b_{ij}^{D}Q_j|e_j(t-\sigma)|\cdot|\mathrm{sign}(e_i(t))|\\
&+\sum_{i=1}^{n}\sum_{j=1}^{n}(\left|\hat{a}_{ij}-\check{a}_{ij}\right|L_j+\left|\hat{b}_{ij}-\check{b}_{ij}\right|M_j)\cdot|\mathrm{sign}(e_i(t))|\\
&+\sum_{i=1}^{n}\sum_{j=1}^{n}|D_{ij}|P_j|(e_j(t-\sigma))|\cdot|\mathrm{sign}(e_i(t))|\\
&+\sum_{i=1}^{n}\sum_{j=1}^{n}|H_{ij}|P_j|(e_j(t-\sigma))|\cdot|\mathrm{sign}(e_i(t))|\\
&-\sum_{i=1}^{n}\delta_i|e_i(t)|-\sum_{i=1}^{n}\omega_i\cdot|\mathrm{sign}(e_i(t))|-\sum_{i=1}^{n}\sum_{j=1}^{n}k_{ij}\left|e_j(t-\sigma)\right|\cdot\mathrm{sign}(e_i(t))\\
&-\sum_{i=1}^{n}\Gamma(t,e)\,|e_i(t)|^{1-q}\cdot|\mathrm{sign}(e_i(t))|\\
=&-\sum_{i=1}^{n}(\delta_i+c_i(t)-\sum_{j=1}^{n}a_{ji}^{D}P_j)|e_i(t)|\\
&-\sum_{i=1}^{n}(\omega_i-\sum_{j=1}^{n}\left|\hat{a}_{ij}-\check{a}_{ij}\right|L_j-\sum_{j=1}^{n}\left|\hat{b}_{ij}-\check{b}_{ij}\right|M_j)\cdot|\mathrm{sign}(e_i(t))|\\
&-\sum_{i=1}^{n}\sum_{j=1}^{n}(k_{ij}-b_{ij}^{D}Q_j-|D_{ij}|P_j-|H_{ij}|P_j)|(e_j(t-\sigma)|\cdot|\mathrm{sign}(e_i(t))|\\
&-\sum_{i=1}^{n}\Gamma(t,e)\,|e_i(t)|^{1-q}\cdot|\mathrm{sign}(e_i(t))|, \qquad (28)
\end{aligned}
$$

$$
\Gamma(t,e)=l\exp\left(\left(\sum_{i=1}^{n}e_i(t)\right)^{q}\right).
$$

When conditions (i)–(iii) are met,then

$$\begin{aligned}\frac{dV(t)}{dt} \leq & -\sum_{i=1}^{n}\Gamma(t,e)\,|e_i(t)|^{1-q}\cdot|\mathrm{sign}(e_i(t))| \\ & -\sum_{i=1}^{n} l\exp((\sum_{i=1}^{n}e_i(t))^q)|e_i(t)|^{1-q}\cdot|\mathrm{sign}(e_i(t))| \\ & -\sum_{i=1}^{n} l\exp((\sum_{i=1}^{n}e_i(t))^q)|e_i(t)|^{1-q}, \\ \sum_{i=1}^{n}|e_i(t)|^{1-q} \geq & (\sum_{i=1}^{n}|e_i(t)|)^{1-q} = V^{1-q},\end{aligned} \tag{29}$$

and, therefore,

$$\frac{dV(t)}{dt} \leq -l\exp\left(V^q\right)V^{1-q},$$

$$\Gamma(t_0,e_0) \leq t_0 + \Gamma_2^{max}, \Gamma_2^{max} = \frac{1}{ql}.$$

Hence, ReSy (10) is synchronized with DrSy (1) in a fixed time under control strategy (18). The proof is complete. □

Remark 3.2. *FinTS and FixTS can both achieve synchronization between DRS within a finite time, but they have fundamental differences in theory and application. The convergence time for FinTS depends on InSts, ensuring synchronization within a finite time, but the convergence time cannot be uniformly estimated. In contrast, FixTS completes synchronization within a uniform upper bound that is independent of InSts. FinTS is suitable for systems with known or controllable InSts, where controller design is relatively simple. However, it has unstable convergence times when faced with disturbances or frequent resets, making it less feasible in engineering applications. On the other hand, FixTS is more suitable for high-demand scenarios like aerospace and smart grids, where time and safety are critical, despite its more complex controller design.*

Remark 3.3. *In this work, a switched discontinuous StFC is designed, which facilitates the achievement of FixTS. The inclusion of switched discontinuous terms effectively addresses the variability and uncertainty of Filippov solutions in the DRS. Naturally, switched discontinuous controllers also have drawbacks: they are prone to inducing oscillations, where even minor parameter perturbations may trigger such oscillatory behavior, which is detrimental to synchronization performance. This issue can be mitigated using optimization algorithms or by approximating the discontinuous functions with continuous ones.*

Remark 3.4. *Reference [40] investigates the predetermined-time stability of memristive chaotic systems, while our study focuses on the FixTS problem of neural networks. In the controller design presented in [40], intermittent control is used, whereas our approach employs a switched StFC. Additionally, the fuzzy method applied in the two studies differs: Reference [40] utilizes the T-S fuzzy method, whereas we adopt the fuzzy 'AND' and fuzzy 'OR' methods.*

Remark 3.5. *In Reference [41], the FixTS of fuzzy complex networks incorporating reaction-diffusion factors is studied, where intermittent control is used to achieve synchronization. The method employed involves power functions and sign functions, whereas our approach utilizes a special exponential function method to achieve FixTS.*

4. Numerical examples

This section presents two numerical examples to validate the viability of the FixTS strategy introduced in the preceding section.

Example 4.1. *Consider the 2-D TDFMNNs (1) as the DrSy, and system (10) as the ReSy with parameters:* $c_1(t) = c_2(t) = 1, I_1 = I_2 = sin(8t), D_{11} = D_{12} = D_{21} = D_{22} = H_{11} = H_{12} = H_{21} = H_{22} = 2, \sigma = 1, L_j = \frac{1}{2}, M_j = \frac{1}{4}, P_j = \frac{1}{2}, Q_j = \frac{1}{4}$.

The neuron activations are defined as

$$\begin{aligned}&\mathcal{F}_j(x) = 0.5\tanh(x),\\ &\mathcal{G}_j(x) = 0.25\tanh(x),\\ &0.5|x-y| \geq |\mathcal{F}_j(x) - \mathcal{F}_j(y)|,\\ &0.25|x-y| \geq |\mathcal{G}_j(x) - \mathcal{G}_j(y)|.\end{aligned}$$

The InSts of the DrSy of (1) is given as

$$\phi(s) = (-2, 3)^T, s \in [-1, 0].$$

The InSts of the ReSy of (10) is given as

$$\Psi(s) = (1, -0.6)^T, s \in [-1, 0].$$

The memristor-based weights are given as follows:

$$a_{11}(x_1(t)) = \begin{cases}-2, & |x_1(t)| \leq 0.8,\\ -1, & |x_1(t)| > 0.8,\end{cases} \quad a_{12}(x_1(t)) = \begin{cases}-1, & |x_1(t)| \leq 0.8,\\ -1.5, & |x_1(t)| > 0.8,\end{cases}$$

$$a_{21}(x_2(t)) = \begin{cases}-1.2, & |x_2(t)| \leq 0.8,\\ -0.5, & |x_2(t)| > 0.8,\end{cases} \quad a_{22}(x_2(t)) = \begin{cases}1.5, & |x_2(t)| \leq 0.8,\\ 0.5, & |x_2(t)| > 0.8.\end{cases}$$

$$b_{11}(x_1(t)) = \begin{cases}-3, & |x_1(t)| \leq 0.8,\\ -2, & |x_1(t)| > 0.8,\end{cases} \quad b_{12}(x_1(t)) = \begin{cases}-2, & |x_1(t)| \leq 0.8,\\ -1, & |x_1(t)| > 0.8,\end{cases}$$

$$b_{21}(x_2(t)) = \begin{cases}-2.5, & |x_2(t)| \leq 0.8,\\ -1, & |x_2(t)| > 0.8.\end{cases} \quad b_{22}(x_2(t)) = \begin{cases}0.5, & |x_2(t)| \leq 0.8,\\ 1, & |x_2(t)| > 0.8.\end{cases}$$

Choosing $\delta_1 = 2, \delta_2 = 2, \omega_1 = 5, \omega_2 = 4, k_{11} = k_{12} = k_{21} = k_{22} = 4, l = 1, q = 0.5$*, and* $u_i(t)$ *gives the following design:*

$$\delta_1 + c_1(t) - \sum_{j=1}^{2} a_{j1}^{D} P_j = 1.4 \geq 0,$$

$$\delta_2 + c_2(t) - \sum_{j=1}^{2} a_{j2}^{D} P_j = 1.5 \geq 0,$$

$$\omega_1 - \sum_{j=1}^{2} \left|\hat{a}_{1j} - \check{a}_{1j}\right| L_j - \sum_{j=1}^{2} \left|\hat{b}_{1j} - \check{b}_{1j}\right| M_j = 3.75 \geq 0,$$

$$\omega_2 - \sum_{j=1}^{2} \left|\hat{a}_{2j} - \check{a}_{2j}\right| L_j - \sum_{j=1}^{2} \left|\hat{b}_{2j} - \check{b}_{2j}\right| M_j = 2.65 \geq 0,$$

$$k_{11} - b_{11}^{D} Q_j - |D_{11}| P_j - |H_{11}| P_j = 1.25 \geq 0,$$

$$k_{21} - b_{21}^{D} Q_j - |D_{21}| P_j - |H_{21}| P_j = 1.375 \geq 0,$$

$$k_{12} - b_{12}^{D} Q_j - |D_{12}| P_j - |H_{12}| P_j = 1.5 \geq 0,$$

$$k_{22} - b_{22}^{D} Q_j - |D_{22}| P_j - |H_{22}| P_j = 1.75 \geq 0.$$

As of right now, it is easily obtained that all circumstances (i)–(iii) in Theorem 3.1 are satisfied.

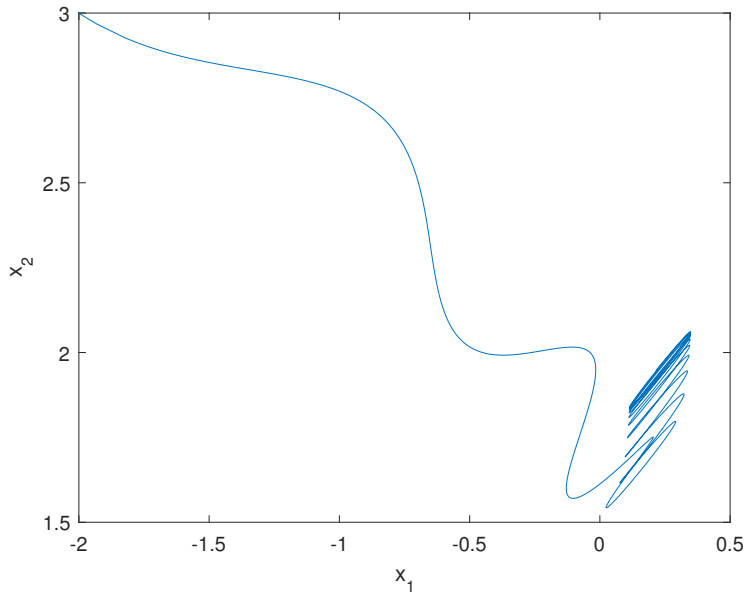

Figure 1. Phase plane of $x_1(t)$ and $x_2(t)$ for DrSy (1) in Example 4.1.

Due to this, in a fixed time, Eqs (1) and (10) can synchronize robustly. Moreover, from Theorem 3.1, Γ^{max} can be determined as follows:

$$\Gamma(t_0, e_0) \leq t_0 + \Gamma_2^{max}, \Gamma_2^{max} = \frac{1}{ql} = \frac{1}{0.5} = 2.$$

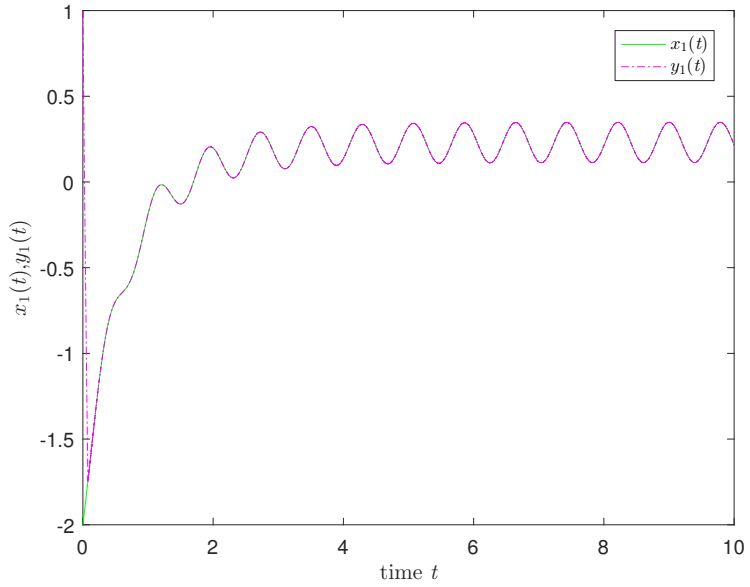

Figure 2. System states $x_1(t)$, $y_1(t)$ with control protocol in Example 4.1.

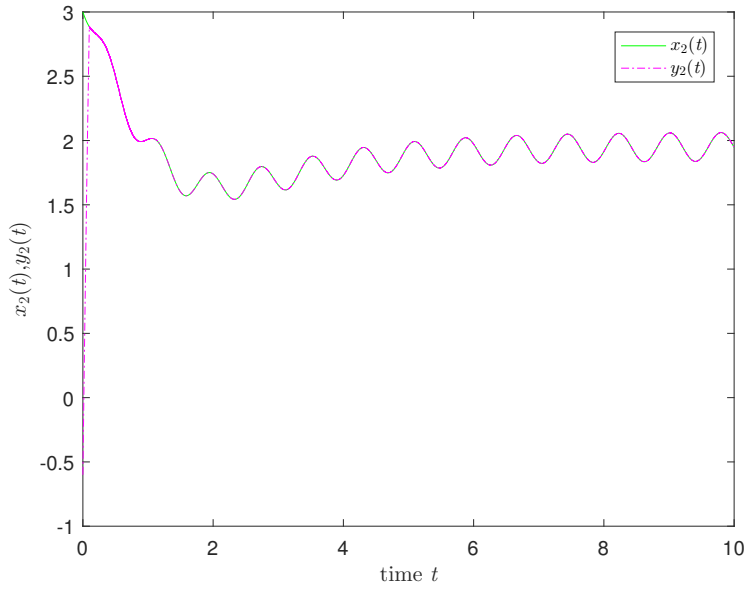

Figure 3. System state $x_2(t)$, $y_2(t)$ with control protocol in Example 4.1.

A numerical simulation is performed utilizing the MATLAB 2020B software to validate the theories. The phase-plane behavior of the TDFMNNs without the controller is shown in Figure 1 for the system's StVas, $x_1(t)$ and $x_2(t)$. Figures 2 and 3 illustrate the states of $x_1(t), y_1(t)$ and $x_2(t), y_2(t)$, respectively, under the controller's action for the controlled TDFMNNs system. Furthermore, Figure 4 illustrates the trajectories of the synchronization errors between the DrSy and the ReSy. It is evident from Figure

4 that the state of the ReSy, propelled by the synchronous controller, converges to that of the DrSy, with the convergence error remaining zero after Γ^{max}. This observation confirms the effectiveness of the proposed controller in driving the system to achieve FixTS.

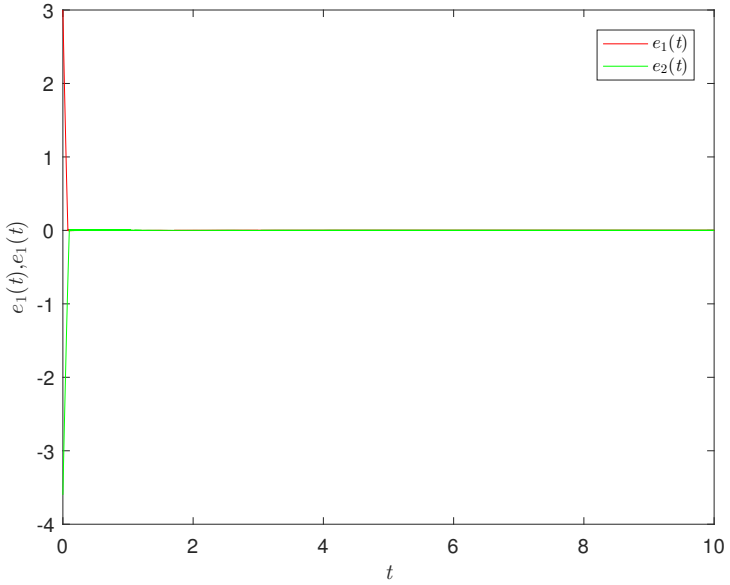

Figure 4. Synchronization error trajectories of DrSy (1) and corresponding ReSy(10) under the control strategy(18) in Example 4.1.

Example 4.2. *Consider a 3-D TDFMNNs described by system (1) as the DrSy and system (10) as the ReSy with parameters* $c_1(t) = c_2(t) = c_3(t) = 1, I_1 = I_2 = I_3 = cos(12t), D_{ij} = H_{ij} = \frac{1}{10}, \sigma = 1, L_j = \frac{3}{5}, M_j = \frac{3}{5}, P_j = \frac{1}{5}, Q_j = \frac{1}{5}$.

The neuron activations are defined as

$$\begin{aligned}
&\mathcal{F}_j(x) = \frac{1}{5}\tanh(x) + \frac{2}{5},\\
&0.2|x - y| \geq |\mathcal{F}_j(x) - \mathcal{F}_j(y)|,\\
&\mathcal{G}_j(x) = \frac{1}{5}\tanh(x) + \frac{2}{5},\\
&0.2|x - y| \geq |\mathcal{G}_j(x) - \mathcal{G}_j(y)|.
\end{aligned}$$

The InSts of the DrSy of (1) is given as

$$\phi(s) = (-\frac{5}{2}, \frac{3}{2}, 1)^T, s \in [-1, 0].$$

The InSts of the ReSy of (10) is given as

$$\Psi(s) = (2, 3, -3)^T, s \in [-1, 0].$$

The memristor-based weights are as follows:

$$a_{11}(x_1(t)) = \begin{cases} -0.1, & |x_1(t)| \le 0.3, \\ -0.3, & |x_1(t)| > 0.3, \end{cases} \quad a_{12}(x_1(t)) = \begin{cases} -0.2, & |x_1(t)| \le 0.3, \\ -0.3, & |x_1(t)| > 0.3, \end{cases}$$

$$a_{13}(x_1(t)) = \begin{cases} -0.4, & |x_1(t)| \le 0.3 \\ -0.3, & |x_1(t)| > 0.3 \end{cases}$$

$$a_{21}(x_2(t)) = \begin{cases} 0.7, & |x_2(t)| \le 0.3, \\ 0.2, & |x_2(t)| > 0.3, \end{cases} \quad a_{22}(x_2(t)) = \begin{cases} 0.7, & |x_2(t)| \le 0.3, \\ 0.4, & |x_2(t)| > 0.3, \end{cases}$$

$$a_{23}(x_2(t)) = \begin{cases} 0.6, & |x_2(t)| \le 0.3, \\ 0.3, & |x_2(t)| > 0.3, \end{cases}$$

$$a_{31}(x_3(t)) = \begin{cases} 0.4, & |x_3(t)| \le 0.3, \\ 0.3, & |x_3(t)| > 0.3, \end{cases} \quad a_{32}(x_3(t)) = \begin{cases} 0.5, & |x_3(t)| \le 0.3, \\ 0.2, & |x_3(t)| > 0.3, \end{cases}$$

$$a_{33}(x_3(t)) = \begin{cases} 0.3, & |x_3(t)| \le 0.3, \\ 0.8, & |x_3(t)| > 0.3, \end{cases}$$

$$b_{11}(x_1(t)) = \begin{cases} 0.3, & |x_1(t)| \le 0.3, \\ 0.2, & |x_1(t)| > 0.3, \end{cases} \quad b_{12}(x_1(t)) = \begin{cases} 0.5, & |x_1(t)| \le 0.3, \\ 0.1, & |x_1(t)| > 0.3, \end{cases}$$

$$b_{13}(x_1(t)) = \begin{cases} 0.2, & |x_1(t)| \le 0.3, \\ 0.8, & |x_1(t)| > 0.3, \end{cases}$$

$$b_{21}(x_2(t)) = \begin{cases} 0.2, & |x_2(t)| \le 0.3, \\ 0.6, & |x_2(t)| > 0.3, \end{cases} \quad b_{22}(x_2(t)) = \begin{cases} 0.3, & |x_2(t)| \le 0.3, \\ 0.5, & |x_2(t)| > 0.3, \end{cases}$$

$$b_{23}(x_2(t)) = \begin{cases} 0.4, & |x_2(t)| \le 0.3, \\ 0.2, & |x_2(t)| > 0.3, \end{cases}$$

$$b_{31}(x_3(t)) = \begin{cases} -0.5, & |x_3(t)| \le 0.3, \\ -0.3, & |x_3(t)| > 0.3, \end{cases} \quad b_{32}(x_3(t)) = \begin{cases} -0.4, & |x_3(t)| \le 0.3, \\ -0.2, & |x_3(t)| > 0.3, \end{cases}$$

$$b_{33}(x_3(t)) = \begin{cases} -0.5, & |x_3(t)| \le 0.3, \\ -1.5, & |x_3(t)| > 0.3. \end{cases}$$

Choosing $\delta_1 = 3, \delta_2 = 3, \delta_3 = 3, \omega_1 = 5, \omega_2 = 5, \omega_3 = 5, k_{ij} = 4, l = 1, q = 0.5$*, and* $u_i(t)$ *gives the following design:*

$$\delta_1 + c_1(t) - \sum_{j=1}^{3} a_{j1}^{D} P_j = 3.72 \geq 0,$$

$$\delta_2 + c_2(t) - \sum_{j=1}^{3} a_{j2}^{D} P_j = 3.7 \geq 0,$$

$$\delta_3 + c_3(t) - \sum_{j=1}^{3} a_{j3}^{D} P_j = 3.64 \geq 0,$$

$$\omega_1 - \sum_{j=1}^{3} \left|\hat{a}_{1j} - \check{a}_{1j}\right| L_j - \sum_{j=1}^{3} \left|\hat{b}_{1j} - \check{b}_{1j}\right| M_j = 4.1 \geq 0,$$

$$\omega_2 - \sum_{j=1}^{3} \left|\hat{a}_{2j} - \check{a}_{2j}\right| L_j - \sum_{j=1}^{3} \left|\hat{b}_{2j} - \check{b}_{2j}\right| M_j = 3.86 \geq 0,$$

$$\omega_3 - \sum_{j=1}^{3} \left|\hat{a}_{3j} - \check{a}_{3j}\right| L_j - \sum_{j=1}^{3} \left|\hat{b}_{3j} - \check{b}_{3j}\right| M_j = 3.62 \geq 0,$$

$$k_{11} - b_{11}^{D} Q_j - |D_{11}| P_j - |H_{11}| P_j = 3.9 \geq 0,$$
$$k_{12} - b_{12}^{D} Q_j - |D_{12}| P_j - |H_{12}| P_j = 3.86 \geq 0,$$
$$k_{13} - b_{13}^{D} Q_j - |D_{13}| P_j - |H_{13}| P_j = 3.8 \geq 0,$$
$$k_{21} - b_{21}^{D} Q_j - |D_{21}| P_j - |H_{21}| P_j = 3.84 \geq 0,$$
$$k_{22} - b_{22}^{D} Q_j - |D_{22}| P_j - |H_{22}| P_j = 3.86 \geq 0,$$
$$k_{23} - b_{23}^{D} Q_j - |D_{23}| P_j - |H_{23}| P_j = 3.88 \geq 0,$$
$$k_{31} - b_{31}^{D} Q_j - |D_{31}| P_j - |H_{31}| P_j = 3.86 \geq 0,$$
$$k_{32} - b_{32}^{D} Q_j - |D_{32}| P_j - |H_{32}| P_j = 3.88 \geq 0,$$
$$k_{33} - b_{33}^{D} Q_j - |D_{33}| P_j - |H_{33}| P_j = 3.66 \geq 0.$$

As of right now, it is easily obtained that Theorem 3.1's requirements (conditions (i)–(iii)) are all met.

Consequently, DrSy (1) in a fixed time effectively accomplished robust synchronization with ReSy (10). Additionally, Theorem 3.1 provides a means to determine Γ^{max} as

$$\Gamma(t_0, e_0) \leq t_0 + \Gamma_2^{max}, \Gamma_2^{max} = \frac{1}{ql} = \frac{1}{0.5} = 2.$$

Figure 5 illustrates the 3-D phase plane characteristics of the StVas $x_1(t), x_2(t)$, and $x_3(t)$ for the uncontrolled TDFMNNs. Similarly, the trajectories of the controlled TDFMNNs system states are shown in Figures 6–8, respectively. The controlled system's trajectories show that the suggested control approach effectively achieves synchronization between DrSy and ReSy. Figure 9 illustrates the controller's performance, demonstrating how the system driven by the synchronous controller reaches the state of DrSy and maintains a convergence error of zero after Γ^{max}.

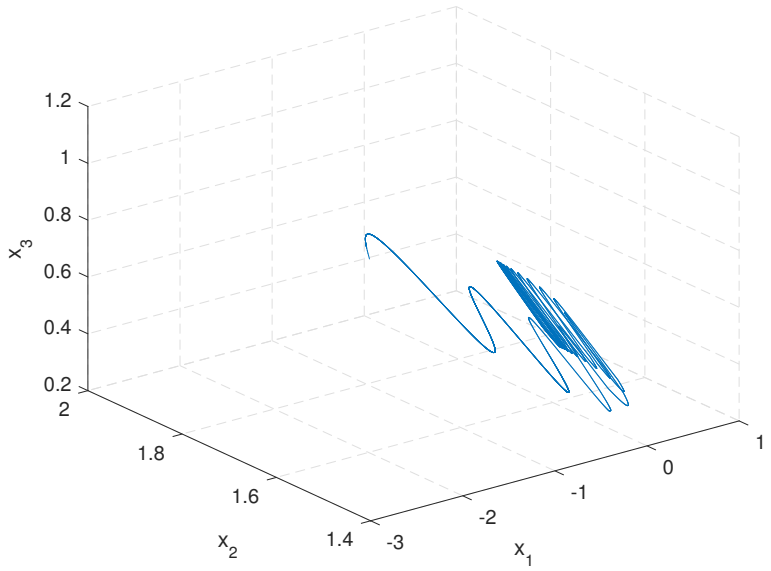

Figure 5. Phase plane of $x_1(t)$, $x_2(t)$, and $x_3(t)$ for DrSy (1) in Example 4.2.

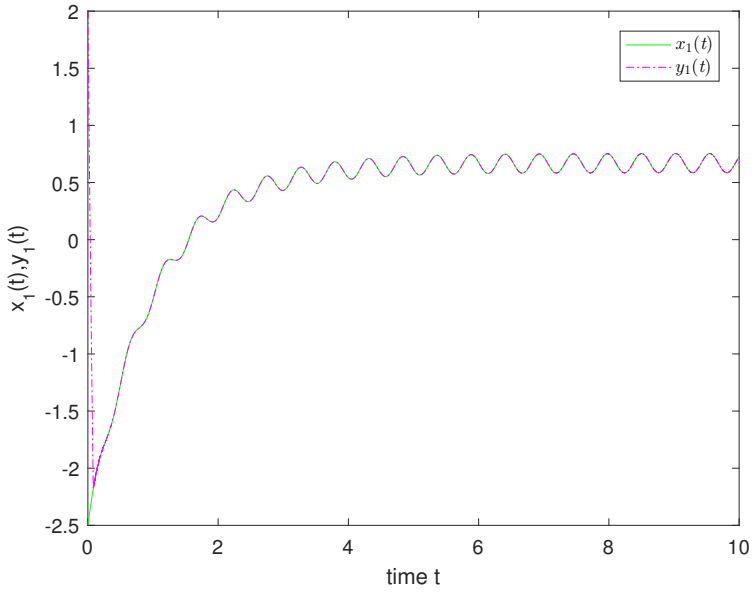

Figure 6. States $x_1(t)$ and $y_1(t)$, with control protocol in Example 4.2.

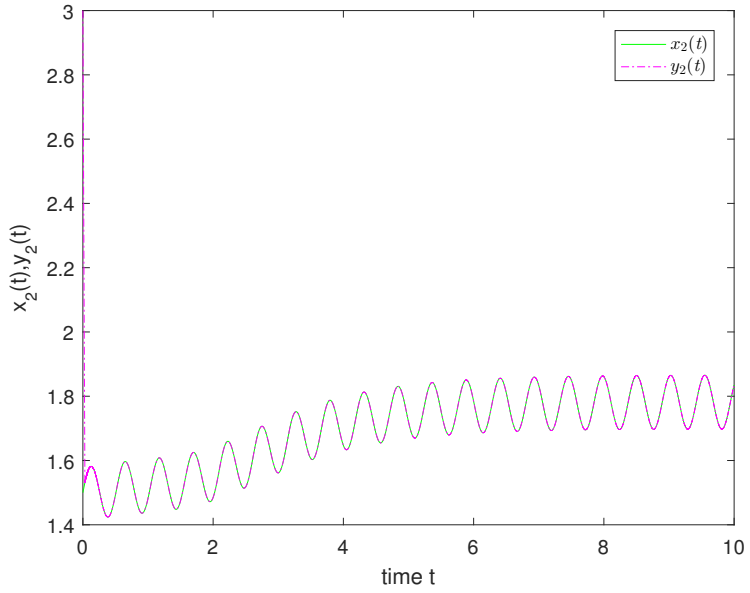

Figure 7. States $x_2(t)$ and $y_2(t)$, with control protocol in Example 4.2.

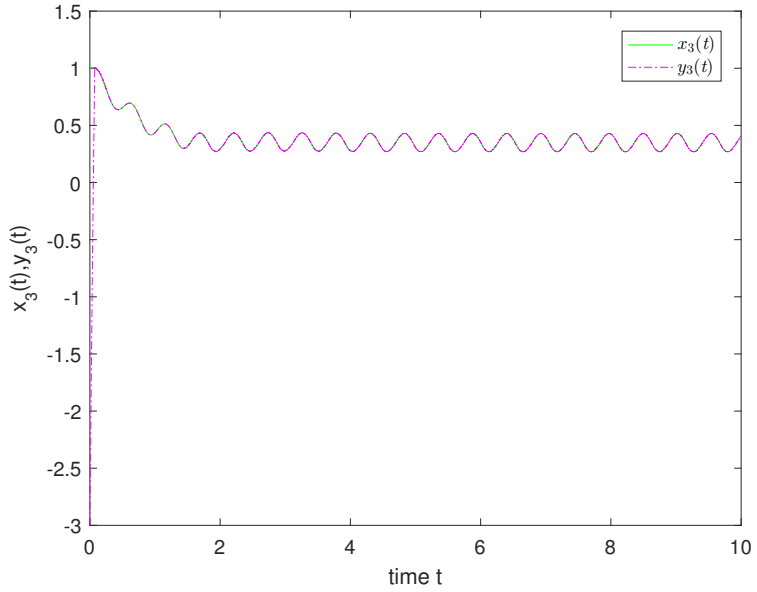

Figure 8. States $x_3(t)$ and $y_3(t)$, with control protocol in Example 4.2.

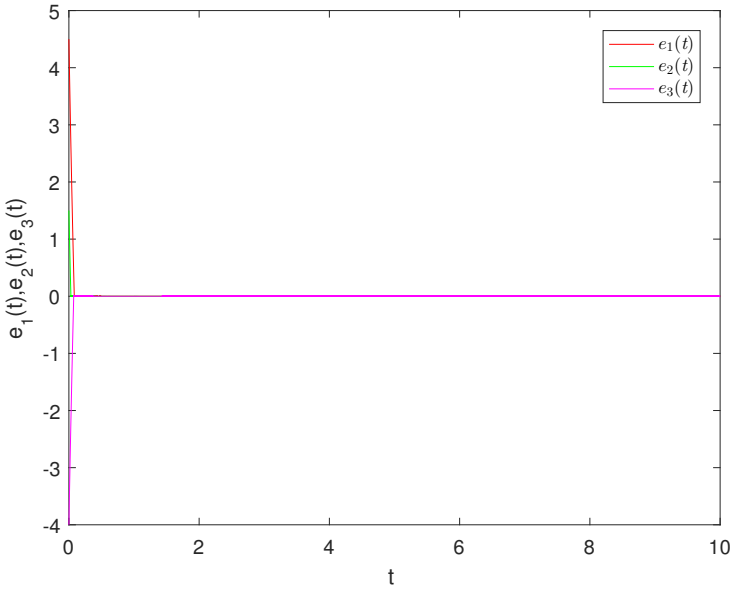

Figure 9. Synchronization error trajectories of DrSy (1) and corresponding ReSy(10) under the control strategy(18) in Example 4.2.

The overall results demonstrate the controller's ability to readily achieve FixTS. Moreover, the simplicity of requiring only three design conditions for obtaining the control rate parameters suggests that the design and estimation of convergence time are less complex, thus affirming the practical feasibility of this optimized controller. In terms of neural network circuit implementation, this optimized controller is also straightforward to implement and incurs lower economic costs. As far as the authors are aware, the neural networks in this paper are constructed considering more objective factors, including memristors, time-variation of coefficients, time-delay, and FL. While previous studies such as [27] investigated FinTS of delayed FNNs with discontinuous activation, and [28] explored FinTS and FixTS, these models do not incorporate memristors. Additionally, although [35] addresses the FixTS problem for MNN, the system in [35] lacks time delay and FL components. Moreover, this paper introduces a modified controller with a special exponential function term, distinct from existing power function form controllers. By employing specially designed exponential functions and leveraging the indefinite derivative Lyapunov function method, a discontinuous StFC is developed to effectively achieve FixTS control of the memristor-based FNNs. Moreover, this approach provides a diversified method for estimating the convergence time, involving very few parameters and offering a simpler formulation for convergence time estimation.

5. Conclusions

This research examines FixTS problems concerning TDFMNNs. To solve these problems, a method that makes use of a special exponential function and Lyapunov function method was adopted. Additionally, a discontinuous StFC was designed, which was able to achieve FixTS while also significantly increasing the convergence rate. In contrast to earlier published literature, FixTS offers several ad-

vantages. First, compared to traditional exponential and asymptotic synchronization, FixTS achieves faster convergence. In contrast, the error states in [12, 18, 42] synchronize over an infinite time horizon, while the FixTS in this paper is achieved within a finite time. Second, the FixTS proposed here also outperforms FinTS. In [43, 44], the convergence time of FinTS heavily affected by the InSts of the system, whereas the convergence time of our FixTS is independent of any InSts. The third advantage lies in the different methods used to achieve FixTS. In [41], fixed-time control is implemented using power and sign functions, while our approach employs a special exponential function to achieve fixed-time control. The control designs in these two approaches are fundamentally different, with our controller having the advantage of fewer control parameters. Although FixTS control can shorten a system's convergence time, they have limitations when the control objective must be reached within a specified, predefined-time frame, independent of the InSts or system factors [45]. For instance, in special engineering applications such as predefined-time altitude control of spacecraft, DC microgrids, aircraft docking, and secure communication, systems must frequently attain specified objectives within a predetermined timeframe by actual requirements [46]. Inspired by [40, 41], predefined-time pinning control of FNNs with reaction-diffusion terms is also a highly significant research topic. We plan to dedicate more time and effort to this area in our future studies.

Use of AI tools declaration

The authors declare they have not used Artificial Intelligence (AI) tools in the creation of this article.

Acknowledgments

This work was supported by Humanity and Social Science Youth foundation of Ministry of Education of China (No. 22YJCZH009), Scientific Research Key Project of Hunan Provincial Education Department (No. 23A0684).

Conflict of interest

The authors declare there is no conflicts of interest.

References

1. L. Chua, Memristor-The missing circuit element, *IEEE Trans. Circuit Theory*, **18** (1971), 507–519. https://doi.org/10.1109/TCT.1971.1083337
2. D. B. Strukov, G. S. Snider, D. R. Stewart, R. S. Williams, The missing memristor found, *Nature*, **453** (2008), 80–83. https://doi.org/10.1038/nature06932
3. S. Wang, L. Song, W. Chen, G. Wang, E. Hao, C. Li, et al., Memristor-based intelligent human-like neural computing, *Adv. Electron. Mater.*, **9** (2023), 1065–1089. https://doi.org/10.1002/aelm.202200877
4. S. P. Adhikari, C. Yang, H. Kim, L. O. Chua, Memristor bridge synapse-based neural network and its learning, *IEEE Trans. Neural Networks Learn. Syst.*, **23** (2012), 1426–1435. https://doi.org/10.1109/TNNLS.2012.2204770

5. H. Sang, Y. Zhao, P. Wang, Y. Wang, S. Yu, G. M. Dimirovski, Finite-time peak-to-peak analysis for switched generalized neural networks comprised of finite-time unstable subnetworks, *Chaos, Solitons Fractals*, **172** (2023), 113555. https://doi.org/10.1016/j.chaos.2023.113555
6. X. W. Zhang, H. N. Wu, Mixed $H2/H_\infty$ stabilization design for memristive neural networks, *Neurocomputing*, **361** (2024), 92–99. https://doi.org/10.1016/j.neucom.2019.07.002
7. I. Ahmad, M. Shafiq, B. Naderi, Finite-time synchronization of four-dimensional memristor-based chaotic oscillator and applied to secure communication systems, *Franklin Open*, **3** (2023), 100015. https://doi.org/10.1016/j.fraope.2023.100015
8. J. Zhang, X. Ma, Y. Li, Q. Gan, C. Wang, Synchronization in fixed/preassigned-time of delayed fully quaternion-valued memristive neural networks via non-separation method, *Commun. Nonlinear Sci. Numer. Simul.*, **113** (2022), 106581. https://doi.org/10.1016/j.cnsns.2022.106581
9. Y. Cao, S. Wang, Z. Guo, T. Huang, S. Wen, Stabilization of memristive neural networks with mixed time-varying delays via continuous/periodic event-based control, *J. Franklin Inst.*, **357** (2020), 7122–7138. https://doi.org/10.1016/j.jfranklin.2020.05.040
10. H. B. Zeng, Y. J. Chen, Y. He, X. M. Zhang, A delay-derivative-dependent switched system model method for stability analysis of linear systems with time-varying delay, *Automatica*, **175** (2025), 112183. https://doi.org/10.1016/j.automatica.2025.112183
11. Y. Chen, C. Lu, X. M. Zhang, Allowable delay set flexible fragmentation approach to passivity analysis of delayed neural networks, *Neurocomputing*, **629** (2025), 129730. https://doi.org/10.1016/j.neucom.2025.129730
12. X. Yao, X. Liu, S. Zhong, Exponential stability and synchronization of Memristor-based fractional-order fuzzy cellular neural networks with multiple delays, *Neurocomputing*, **419** (2021), 239–250. https://doi.org/10.1016/j.neucom.2020.08.057
13. K. Ding, Q. Zhu, Impulsive method to reliable sampled-data control for uncertain fractional-order memristive neural networks with stochastic sensor faults and its applications, *Nonlinear Dyn.*, **100** (2020), 2595–2608. https://doi.org/10.1007/s11071-020-05670-y
14. G. Zhang, J. Qin, Y. Zhang, G. Gong, Z. Y. Xiong, X. Ma, et al., Functional materials for memristor-based reservoir computing: Dynamics and applications, *Adv. Funct. Mater.*, **33** (2023), 2302929. https://doi.org/10.1002/adfm.202302929
15. Q. Gan, L. Li, J. Yang, Y. Qin, M. Meng, Improved results on fixed-/preassigned-time synchronization for memristive complex-valued neural networks, *IEEE Trans. Neural Networks Learn. Syst.*, **33** (2022), 5542–5556. https://doi.org/10.1109/TNNLS.2021.3070966
16. W. Wang, Y. Sun, M. Yuan, Z. Wang, J. Cheng, D. Fan, et al., Projective synchronization of memristive multidirectional associative memory neural networks via self-triggered impulsive control and its application to image protection, *Chaos, Solitons Fractals*, **150** (2021), 150. https://doi.org/10.1016/j.chaos.2021.111110
17. S. Gong, Z. Guo, S. Wen, T. Huang, Finite-time and fixed-time synchronization of coupled memristive neural networks with time delay, *IEEE Trans. Cybern.*, **51** (2021), 2944–2955. https://doi.org/10.1109/TCYB.2019.2953236

18. X. Wu, S. Liu, H. Wang, Asymptotic stability and synchronization of fractional delayed memristive neural networks with algebraic constraints, *Commun. Nonlinear Sci. Numer. Simul.*, **114** (2022), 106694. https://doi.org/10.1016/j.cnsns.2022.106694

19. L. Wang, C. K. Zhang, Exponential synchronization of memristor-based competitive neural networks with reaction-diffusions and infinite distributed delays, *IEEE Trans. Neural Networks Learn. Syst.*, **35** (2022), 745–758. https://doi.org/10.1109/TNNLS.2022.3176887

20. Z. Cai, L. Huang, Finite-time stabilization of delayed memristive neural networks: Discontinuous state-feedback and adaptive control approach, *IEEE Trans. Neural Networks Learn. Syst.*, **29** (2018), 856–868. https://doi.org/10.1109/TNNLS.2017.2651023

21. T. Jia, X. Chen, F. Zhao, J. Cao, J. Qiu, Adaptive fixed-time synchronization of stochastic memristor-based neural networks with discontinuous activations and mixed delays, *J. Franklin Inst.*, **360** (2023), 3364–3388. https://doi.org/10.1016/j.jfranklin.2022.11.006

22. A. Polyakov, Nonlinear feedback design for fixed-time stabilization of linear control systems, *IEEE Trans. Autom. Control*, **57** (2012), 2106–2110. https://doi.org/10.1109/TAC.2011.2179869

23. Q. Liu, H. Yan, H. Zhang, X. Zhan, K. Shi, Intermittent exponential synchronization for memristor-based neural networks with inertial items and mixed time-varying delays, *IEEE Trans. Syst. Man Cybern.: Syst.*, **53** (2022), 2925–2937. https://doi.org/10.1109/TSMC.2022.3220979

24. F. Setoudeh, M. M. Dezhdar, M. Najafi, Nonlinear analysis and chaos synchronization of a memristive-based chaotic system using adaptive control technique in noisy environments, *Chaos, Solitons Fractals*, **164** (2022), 112710. https://doi.org/10.1016/j.chaos.2022.112710

25. F. Wu, Y. Huang, Finite-time synchronization and H_∞ synchronization of coupled complex-valued memristive neural networks with and without parameter uncertainty, *Neurocomputing*, **469** (2022), 163–179. https://doi.org/10.1016/j.neucom.2021.10.067

26. F. Merrikh-Bayat, F. Merrikh-Bayat, S. B. Shouraki The neuro-fuzzy computing system with the capacity of implementation on a memristor crossbar and optimization-free hardware training, *IEEE Trans. Fuzzy Syst.*, **22** (2014), 1272–1287. https://doi.org/10.1109/TFUZZ.2013.2290140

27. L. Duan, H. Wei, L. Huang, Finite-time synchronization of delayed fuzzy cellular neural networks with discontinuous activations, *Fuzzy Sets Syst.*, **361** (2019), 56–70. https://doi.org/10.1016/j.fss.2018.04.017

28. F. Kong, Q. Zhu, R. Sakthivel, Finite-time and fixed-time synchronization control of fuzzy Cohen-Grossberg neural networks, *Fuzzy Sets Syst.*, **394** (2020), 87–109. https://doi.org/10.1016/j.fss.2019.12.002

29. M. S. Aslam, T. Radhika, A. Chandrasekar, Q. Zhu, Improved event-triggered-based output tracking for a class of delayed networked T–S fuzzy systems, *Int. J. Fuzzy Syst.*, **26** (2024), 1247–1260. https://doi.org/10.1007/s40815-023-01664-1

30. F. Liu, W. Meng, R. Lu, Anti-synchronization of discrete-time fuzzy memristive neural networks via impulse sampled-data communication, *IEEE Trans. Cybern.*, **53** (2023), 4122–4133. https://doi.org/10.1109/TCYB.2021.3128903

31. C. Xu, M. Jiang, J. Hu, Fixed-time synchronization of complex-valued memristive competitive neural networks based on two novel fixed-time stability theorems, *Neural Comput. Appl.*, **35** (2023), 22605–22620. https://doi.org/10.1007/s00521-023-08874-6

32. M. Zheng, L. Li, H. Peng, J. Xiao, Y. Yang, Y. Zhang, Fixed-time synchronization of complex-valued memristive competitive neural networks based on two novel fixed-time stability theorems, *IEEE Access*, **6** (2018), 12085–12102. https://doi.org/ 10.1109/ACCESS.2018.2805183

33. P. Wang, X. Li, J. Lu, J. Lou, Fixed-time synchronization of stochastic complex-valued fuzzy neural networks with memristor and proportional delays, *Neural Process. Lett.*, **55** (2023), 8465–8481. https://doi.org/10.1007/s11063-023-11320-2

34. J. Chen, Z. Zeng, P. Jiang, On the periodic dynamics of memristor-based neural networks with time-varying delays, *Inf. Sci.*, **279** (2019), 358–373. https://doi.org/10.1016/j.ins.2014.03.124

35. J. Li, H. Jiang, C. Hu, A. Alsaedi, Finite/fixed-time synchronization control of coupled memristive neural networks, *J. Franklin Inst.*, **356** (2019), 9928–9952. https://doi.org/10.1016/j.jfranklin.2019.09.015

36. Z. Cai, L. Huang, Z. Wang, Fixed/preassigned-time stability of time-varying nonlinear system with discontinuity: Application to Chua's circuit, *IEEE Trans. Circuits Syst. II Express Briefs*, **69** (2022), 2987–2991. https://doi.org/10.1109/TCSII.2022.3166776

37. Z. Cai, L. Huang, Z. Wang, Novel fixed-time stability criteria for discontinuous nonautonomous systems: Lyapunov method with indefinite derivative, *IEEE Trans. Cybern.*, **52** (2022), 4286–4299. https://doi.org/10.1109/TCYB.2020.3025754

38. F. H. Clarke, Y. S. Ledyaev, R. J. Stern, P. R. Wolenski, et al., *Nonsmooth Analysis and Control Theory*, Springer-Verlag, New York, 1990.

39. T. Yang, L. B. Yang, The global stability of fuzzy cellular neural network, *IEEE Trans. Circuits Syst. I: Fundam. Theory Appl.*, **43** (1996), 880–883. https://doi.org/10.1109/81.538999

40. Q. Wang, L. Wang, W. Wen, Y. Li, G. Zhang, Dynamical analysis and preassigned-time intermittent control of memristive chaotic system via T–S fuzzy method, *Chaos*, **35** (2025), 023102. https://doi.org/10.1063/5.0221159

41. X. Hu, L. Wang, C. K. Zhang, Y. He, Fixed-time synchronization of fuzzy complex dynamical networks with reaction-diffusion terms via intermittent pinning control, *IEEE Trans. Fuzzy Syst.*, **52** (2024), 2307–2317. https://doi.org/10.1109/TFUZZ.2024.3349599

42. Y. Cao, Z. Guo, T. Huang, S. Wen, Global exponential synchronization of delayed memristive neural networks with reaction–diffusion terms, *Neural Networks*, **123** (2020), 70–81. https://doi.org/10.1016/j.neunet.2019.11.008

43. L. Chen, M. Gong, Y. Zhao, X. Liu, Finite-time synchronization for stochastic fractional-order memristive BAM neural networks with multiple delays, *Fractal Fract.*, **7** (2023), 678. https://doi.org/10.3390/fractalfract7090678

44. Z. Lu, Q. Ge, Y. Li, J. Hu, Finite-time synchronization of memristor-based recurrent neural networks with inertial items and mixed delays, *IEEE Trans. Syst. Man Cybern, Syst.*, **51** (2021), 2701–2711. https://doi.org/10.1109/TSMC.2019.2916073

45. S. Shao, X. Liu, J. Cao, Prespecified-time synchronization of switched coupled neural networks via smooth controllers, *Neural Networks*, **133** (2021), 32–39. https://doi.org/10.1016/j.neunet.2020.10.007

46. Q. Wang, H. Zhao, A. Liu, L. Li, S. Niu, C. Chen, Predefined-time synchronization of stochastic memristor-based bidirectional associative memory neural networks with time-varying delays, *IEEE Trans. Cognit. Dev. Syst.*, **14** (2022), 1584–1593. https://doi.org/10.1109/TCDS.2021.3126759

AIMS Press